Prepublished copy

Nature Environment & Pollution Technology

This is a peer-reviewed prepublished version of the paper

Original Research

Physico-Chemical, Morphological and Elemental Composition Characterization of Starch Obtained from *Amorphophallus Paeoniifolius* Tuber Corms

Neetu Saharan, Neeraj Wadhwa and Smriti Gaur†

Department of Biotechnology, Jaypee Institute of Information and Technology, Noida, India

†Corresponding author: Smriti Gaur; smritigaurjiit@gmail.com

Key Words	Starch, Gelatinization, Biodegradable, Sustainable, Plasticizers
DOI	https://doi.org/10.46488/NEPT.2026.v25i02.B4374 (DOI will be active only after the final publication of the paper)
Citation for the Paper	Saharan, N., Wadhwa, N. and Gaur, S., 2026. Physico-chemical, morphological and elemental composition characterization of starch obtained from *Amorphophallus paeoniifolius* tuber cormss. *Nature Environment and Pollution Technology*, 25(2), B4374. https://doi.org/10.46488/NEPT.2026.v25i02.B4374

ABSTRACT

This study explores the potential of *Amorphophallus paeoniifolius* starch as a sustainable biopolymer for biodegradable food packaging. The isolated starch exhibited a C-type crystalline structure with 34.3% crystallinity and showed diverse granule morphology and good thermal stability. Proximate composition revealed high starch (78.61 g/100 g) with low ash (0.17 g/100 g) and fat (0.30 g/100 g), supporting its purity and functional suitability. The presence of hydroxyl (-OH) groups further enhanced mechanical cohesion, indicating its ability to form stable biofilms. These results highlight the novelty of utilizing *A. paeoniifolius* starch as an eco-friendly, renewable, and non-toxic material with promising applications in sustainable packaging and coating technologies. These properties the novelty of *A. paeoniifolius* starch as a renewable, biodegradable, and functional biopolymer, supporting its application in sustainable packaging and coating technologies.

1. INTRODUCTION

Elephant Foot Yam (EFY), scientifically known as *Amorphophallus paeoniifolius* (*A. paeoniifolius*) and commonly referred to as "Jameenkand" in Hindi, is a tropical tuber crop extensively cultivated in humid regions across India, Southeast Asia, and Africa (Singh & Wadhwa, 2014; Mukherjee et al., 2014). It belongs to the Araceae family, which comprises around 170 species (Mukherjee et al., 2014). EFY is renowned for its rich nutritional profile and low-fat content. In particular, it is a significant source of essential fatty acids, including Omega-3, which has been shown to positively impact cholesterol levels (Reddy et al., 2014). Additionally, EFY supports estrogen regulation in women, promoting hormonal balance, and thus holds potential as a functional ingredient for enhancing human health.

Polysaccharides such as natural gums, chitosan, alginate, carrageenan, and gellan gum are widely used in coating development due to their functional properties. Among them, starch stands out for its biodegradability, thermoplastic nature, and aesthetic appeal, making it a preferred choice for coatings. Starch is a semi-crystalline, polysaccharide carbohydrate, mainly composed of amylose and amylopectin (Sukhija et al., 2016; Kandekar et al., 2021). Amylose is a linear polymer with chains linked by α-1, 4 bonds, whereas amylopectin is a branched polymer featuring both α-1, 4 and α-1, 6 linkages (Kandekar et al., 2021; Shujun et al., 2005; M et al., 2018). These structural differences are key to starch's wide applications across food and non-food industries (Zhang et al., 2017; Marimuthu et al., 2013). It is commonly derived from sources like corn and potatoes and highly valued for its ease of extraction, cost-effectiveness, and eco-friendly properties, leaving minimal environmental residue (Zhang et al., 2017; M et al., 2018; Theivasanthi & Alagar, 2011).

Resistant starch (RS) is a functional fiber that remains undigested in the small intestine but gets broken down partially or fully in the large intestine, producing short-chain fatty acids (SCFAs) such as butyrate, propionate, and acetate. SCFAs help regulate blood glucose levels, lower the risk of colorectal cancer linked to red meat consumption, enhance lipid oxidation postprandially and promote satiety (Geirnaert et al., 2017). RS has advantages over traditional fibers, including low water-holding capacity, fine particle size, and a neutral flavor. Acting as a prebiotic, RS promotes gut health and supports various physiological functions, including improved fatty acid digestion, reduced inflammation, and better glycemic control (Islam et al., 2022). Resistant starch-rich powder (RSRP) such as those from banana starch improves bakery products by moderating starch availability and slowing carbohydrate release. Research by Baixauli showed that replacing wheat flour with resistant starch from native maize reduced muffin volume, height, and gas cell formation (Abbas et al., 2010). It is also used in microencapsulation of probiotics in dairy products to enhance their viability, as well as in reducing oxidation and odor in fish oil (Awuchi et al., 2022). Furthermore, starch nanoparticles have gained attention for application in food packaging, plastic fillers, as

well as in medical fields for the treatment and diagnosis of cardiovascular diseases and drug delivery systems (Awuchi et al., 2022).

Starch extracted from *A. paeoniifolius* shows broad applicability as a thickener, adhesive, gelling agent, stabilizer, and bulking agent. It is also used as a base material for developing edible coatings, biodegradable packaging films, and active packaging films (Shujun et al., 2006). Its moderate granule size enhances its suitability for film production and food product formulations (Aprianita et al., 2009). In bioplastics, plant-derived starches are preferred for their eco-friendly, abundant, low-cost, and non-toxic characteristics, contributing to advancements in biodegradable plastic technologies (Sukhija et al., 2016; Wahyuningtiyas & Suryanto, 2017). Cassava and sago starches are common in bioplastic and biofilm production respectively, while other sources include corn, peas, oats, potatoes (sweet and white), water chestnuts, wheat, chestnuts, bananas, rye, and tapioca (Wahyuningtiyas & Suryanto, 2017; Sondari et al., 2019; Özdamar & Ateş, 2018). Structural composition of starch plays a key role in determining film properties. Studies suggest that higher amylose content can enhance the coating's mechanical integrity and its resistance to moisture and gas transmission. According to Oyom and co-workers, starch-based edible coatings exhibit excellent gas barrier properties due to hydrogen bond arrangements. They are also odorless and colorless, allowing the permeation of flavoring agents. However, a significant limitation is their low water resistance, resulting from starch's intrinsic hydrophilicity (Oyom et al., 2022).

Natural starch has limited industrial applications due to weak pasting properties and undesirable gel formation upon cooling. To address this, starch is often modified chemically, enzymatically, and via hydrolysis to enhance its water-holding capacity, heat resistance, binding ability, and thickening efficiency. Modified tapioca starch and lecithin improve the texture and overall quality of reduced-fat Feta cheese, while high-amylose cornstarch improves the texture of extruded and fried snacks (Abbas et al., 2010). Additionally, modified starches are employed in biodegradable food packaging films due to their superior physical and mechanical properties (Andrêssa Maria Medeiros Theóphilo Galvão et al., 2018).

Despite the promising attributes of *A. paeoniifolius* starch, there is a limited research focused on its properties. Most studies focus on common sources like maize and potato, with little exploration of the organoleptic, structural, functional, and thermal characteristics of *A. paeoniifolius* starch, which are important for industrial and food applications. Moreover, the effects of processing methods, like alkaline extraction on its quality are not well understood. This study aims to fill these existing research gaps by isolating starch from *A. paeoniifolius* using an alkaline method and characterizing its structural, thermal, and morphological properties. Advanced analytical techniques such as Differential Scanning Calorimetry (DSC), Fourier Transform Infrared Spectroscopy (FTIR), X-ray Diffraction (XRD), Scanning Electron Microscopy (SEM), and Energy Dispersive X-ray Spectroscopy (EDX) will be employed. These analyses

will provide valuable insights into the physicochemical attributes of *A. paeoniifolius* starch and its potential for bio-based film development.

2. MATERIALS AND METHODS

2.1. Materials

In this study, mature corms of *A. paeoniifolius* were sourced from the local market in Modinagar, Ghaziabad, Uttar Pradesh. The corms underwent a thorough cleaning process, which involved washing with purified water to eliminate any surface contaminants, ensuring they were adequately prepared for subsequent experimental procedures.

2.2. Isolation of Starch

The extraction of starch from *A. paeoniifolius* was carried out following the methodologies described by (Sukhija et al., 2016; Kandekar et al., 2021). *A. paeoniifolius* corms were weighed, thoroughly washed, and peeled. These cleaned corms were then chopped into small segments and soaked in a solution containing 0.25% potassium metabisulfite and 0.12% citric acid for 1h. After soaking, the pieces were blended with distilled water for 5 min to form slurry. The resulting slurry was filtered through muslin cloth to eliminate the fibrous material from the starch suspension. The filtrated solution was kept at 4°C for 4 h, allowing the starch to settle at the bottom. After sedimentation, the clear supernatant was gently poured off and the starch sediment was resuspended in water and treated with a 0.2% sodium hydroxide (NaOH) solution. The washing step was carried out multiple times to ensure the removal of impurities and obtained purified starch. Finally, the starch was dried at a temperature 45°C –50°C for 3–4 h, ground into a fine powder, and stored in an airtight container at room temperature until further analysis.

2.3. Organoleptic and Physicochemical Properties of Starch

2.3.1. Iodine Test, Organoleptic Properties and pH

The iodine test for starch was performed by adding 2 drops of iodine solution to 2 mL of a 5% starch solution, and then the mixture was gently mixed and warmed in a water bath for few minutes. For the organoleptic properties of starch, the color, odour, taste, and texture were carefully observed and documented. The pH of the starch samples was determined by preparing a slurry containing 1 g of starch powder in 30 mL of distilled water, measuring the pH using a calibrated pH meter under room temperature [25°C -30°C] (Yusuf et al., 2022). The starch yield percentage was determined using Equation 1 as follows:

$$\text{Starch yield (\%)} = \frac{\text{Weight of extracted starch}}{\text{Weight of } A.\ paeoniifolius} \times 100 \quad (1)$$

2.4. Proximate /Chemical Composition Analysis of Starch

The proximate and chemical compositions of *A. paeoniifolius* starch were analyzed in accordance with standardized protocols at an International Organization for Standardization (ISO) and Food Safety and Standards Authority of India (FSSAI) certified laboratory (Advanced Research & Analytical Services, Ghaziabad, Uttar Pradesh, India). Moisture, ash, and starch contents were determined as per (IS 4706-2) (Bureau of Indian Standards (BIS), 1978), while protein content was quantified using the Kjeldahl method (IS 7219-1973), with a conversion factor of 6.25 applied to calculate the protein content. Fat content was estimated using the Soxhlet extraction method (IS 4684-1975), and sugar content was measured according to IS 2650-1975. Carbohydrate content was determined following IS 1656-2022 and energy content was computed from the proximate composition as per IS 9487-1981. Dietary fiber was quantified gravimetrically using the methodology outlined in IS 11062-2019.

2.5. Fourier Transform Infrared Spectroscopy (FTIR)

The functional characterization of *A. paeoniifolius* starch granules was performed using FTIR spectroscopy on a Shimadzu FTIR Spectrophotometer (Japan) at the Department of material characterization laboratory, Jaypee Institute of Information Technology, Noida. A finely powdered starch sample was thoroughly combined with spectroscopic grade potassium bromide (KBr) in a 1:100 proportion to obtain a homogeneous mixture for FTIR analysis. KBr being spectroscopically inert was selected to facilitate the formation of translucent pellets that allow effective transmission of infrared light. The combination was then compressed into a translucent pellet using a hydraulic press under high pressure. Spectral data were recorded in the wavenumber range of 4000–400 cm^{-1}, enabling precise identification of functional groups and molecular interactions (Marichelvam et al., 2019).

2.6. Thermal Analysis Using Differential Scanning Calorimetry (DSC)

The thermal behaviour of the starch was analyzed using DSC. For this analysis, a 5 mg starch sample was accurately weighed and placed into a DSC sample pan. The analysis of the starch granules was carried out using a HITACHI DSC 7000 system, operated with a computerized analyzer at the Department of material characterization laboratory, Jaypee Institute of Information Technology, Noida. The scanning was conducted under a nitrogen atmosphere, applying a constant heating rate of 10°C per minute, across a temperature range of 30°C to 160°C (Kandekar et al., 2021; Esquivel-Fajardo et al., 2022).

2.7. Morphological Characterization of Starch by Scanning Electron Microscopy (SEM)

The surface morphology of *A. paeoniifolius* starch granules was examined using SEM with a ZEISS EVO40 microscope at Jawaharlal Nehru University, New Delhi. For SEM preparation, isolated starch samples were gently dusted onto double-sided adhesive carbon tape, which was mounted on aluminum stubs to ensure stable adhesion. The samples were then sputter coated with a thin layer of gold to enhance conductivity. Imaging was conducted with an accelerating voltage of 20 kV, enabling detailed visualization of the starch granule structures. This methodological approach facilitated high resolution imaging, revealing critical insights into the granule morphology and surface characteristics (Sukhija et al., 2016; Wahyuningtiyas & Suryanto, 2017).

2.8. Energy Dispersive X-Ray Spectroscopy (EDX)

In this analysis, a starch sample was subjected to X-ray bombardment, causing the emission of characteristic X-rays specific to each element present. These emitted X-rays were subsequently detected and analyzed using an EDX detector at Jawaharlal Nehru University, New Delhi. The resulting spectrum provided a detailed compositional profile, identifying key elements within the alloy, such as Carbon (C), Oxygen (O), and Hydrogen (H), as indicated by spectral peaks in accordance with referenced studies (Sukhija et al., 2016; Wahyuningtiyas & Suryanto, 2017).

2.9. X-Ray Diffraction (XRD)

XRD analysis of the starch sample was conducted at the Department of material characterization laboratory, Jaypee Institute of Information Technology, Noida. The analysis utilized an X-ray diffractometer equipped with a Cu-Kα radiation source (wavelength equals to 1.54056 Å). The device operated under a voltage of 40 kV and a current of 30 mA. The scanning procedure covered 2θ range of 10° to 80°, aimed at investigating the structure of starch. Data were collected in continuous scan mode with a scanning speed of 2.0° per minute and a 15 mm receiving slit was used to ensuring high-resolution diffraction patterns. This setup provided a detailed examination of the crystallographic properties of the starch sample (Theivasanthi & Alagar, 2011).

3. RESULTS AND DISCUSSION

3.1. Assessing Starch Yield and Its Physicochemical and Organoleptic Properties

The percentage yield of starch extracted from *A. paeoniifolius* was determined to be 1.2%, with 6 g of starch recovered from 500 g of fresh tubers. These results revealed the variation in starch content among different tuber sources, highlighting the significant influence of tube type on starch extraction efficiency.

The starch obtained from *A. paeoniifolius* tested positive for the iodine test, exhibited a white color, had fine texture, was odorless, tasteless, and was insoluble in both water and alcohol, and had a pH of 6.10. Similar findings have been reported by Yusuf et al., 2022, where the iodine test for the native and silicified starch samples obtained from *Ipomoea batatas* was also positive. The color of their samples was white, and both native as well as silicified samples were noted to be odorless, tasteless, and had a fine texture. A study done by Jubril et al., 2012 reported that phosphate starch, pregelatinized starch, and sweet potato starch powders turned blue-black upon the addition of iodine solution, further confirming the presence of starch.

3.2. Proximate and Chemical Composition Analysis

Proximate composition is reliable method for assessing starch purity, where more starch and less protein, fat, ash, and fiber are preferred. Excess protein and fat can affect swelling and pasting properties by interacting with starch granules and reducing gelatinization (Schoch, 1968; Olkku & Rha, 1978; Yang & Chang, 1999; Liang & King, 2003; Lumdubwong & Seib, 2000). Previous study showed that protein can changes the gelatinization and pasting behavior of starch highlighting its significant role in functionality (Hamaker & Griffin, 1993). Therefore, proximate and chemical analyses are essential to evaluate the fundamental composition of food or agricultural products. The result for isolated starch from *A. paeoniifolius*is summarized in Table 1.

Table 1: Proximate/chemical analysis of *Amorphophallus paeoniifolius* starch.

Test Parameters	Value (g/100g)	Test Method
Moisture	11.8	IS:4706
Total Ash	0.17	IS:4706
Starch	78.61	IS:4706
Protein	6.76	IS:7219
Total fat	0.30	IS:4684
Total sugar	BDL(DL-0.5)	IS:2650
Carbohydrate	81.19	IS:1656
Dietary Fiber	2.58	IS: 11062
Energy	354.50 Kcal/100g	IS:9487

3.2.1. Analysis of Moisture Content

Moisture content plays a critical role in determining the texture, stability, and application performance of starch. Excess moisture can cause clumping, while insufficient moisture may lead to brittleness, In this study, *A. paeoniifolius* starch showed a moisture content 11.8%, which falls within the range reported for

purple-fleshed sweet potato (PFSP) (8.52% and 14.86%) (Julianti et al., 2018). Variability in starch moisture depends on factors such as the drying conditions and seed structure (Andrabi et al., 2016;Kaur & Sandhu, 2010). Lower moisture enhances storage stability by reducing microbial activity (Alozie et al., 2009). The relatively low moisture content observed here suggests better shelf-life and reduced microbial contamination risk.

3.2.2. Analysis of Ash Content

Ash content indicates total mineral residue after the combustion of organic matter. In this study *A. paeoniifolius* starch, ash content was 0.17% which is low and comparable to purple-fleshed sweet potato (PFSP) starch, (0.26% and 0.36% Julianti et al., 2018). Such low ash value suggests minimal mineral impurities desirable for applications requiring high-purity starch.

3.2.3. Analysis of Fat Content

Fats play an important role in food systems by providing energy, enhancing flavor, and influencing storage stability of flour-based products (Titov, 2012; Levitsky et al., 2020; Boahemaa et al., 2024). The fat content of *A. paeoniifolius* starch was 0.30% determined by Soxhlet technique. This value is lower than PFSP starch, (Julianti et al., 2018).), reflecting minimal lipid presence. Such low-fat content is advantageous for storage stability and for applications requiring starch with reduced lipids.

3.2.4. Analysis of Dietary Fiber

Dietary fiber (DF) refers to non-digestible plant components that are partially or fully fermented in the large intestine. It plays an important role in functional foods and contributes to health benefits such as lowering blood sugar and lipid levels, and reducing risks of gastrointestinal disorders (He et al., 2022; Boahemaa et al., 2024). In this study, *A. paeoniifolius* starch showed a dietary fiber content of 2.58%, which falls within the range reported for purple-fleshed sweet potato (0.25–2.59%, Julianti et al., 2018). The low DF content confirms its predominance as a carbohydrate source with minimal fiber residue.

3.2.5. Analysis of Carbohydrate and Energy

Carbohydrates are the major source of dietary energy and structural components of living organisms (Cummings & Stephen, 2007; Witek et al., 2022). In this study, *A. paeoniifolius* starch contained 81.19% carbohydrates, similar to taro (77.82–86.11%) and yam (75.98–84.07%) (Ijarotimi et al., 2015; Kibret Akalu & Haile Geleta, 2019), but higher than sweet potato (20.28–35.12%) (Omodamiro et al., 2013). Its calculated energy value (354.50 Kcal/100 g) was also comparable with other root starches, supporting its

role as an energy-dense food source. Sugar content was below detection limit (<0.5 g), consistent with Meludu (2010).

3.2.6. Analysis of Starch Content

Starch is the major storage polysaccharide in plants and a key dietary carbohydrate (Omar et al., 2016). In *A. paeoniifolius* corms, starch content was 78.61%, higher than PFSP (50.20–62.93%) (Julianti et al., 2018) but within the range reported for other tubers (92–96%) (Abegunde, 2012). The overall composition—high starch (78.61%), low ash (0.17%), low fat (0.30%), and moderate fiber (2.58%)—suggests suitability for biofilm formation, where starch provides structural integrity and reduced mineral and lipid contents enhance mechanical and barrier properties.

3.2.7. Analysis of Protein Content

Protein is an essential nutrient that not only supports human health but also influences functional properties such as water and oil absorption, gelation, and rheology, which are critical in food product development (Boahemaa et al., 2024). Plant-derived proteins, such as those from soy, rice, and wheat, have been shown to promote gut health and microbial balance (Ashaolu, 2020; Huang et al., 2016).

In this study, the protein content of *A. paeoniifolius* was found to be 6.76%, as determined by using the Kjeldahl method. The presence of moderate protein in *Amorphophallus* starch may enhance certain functional properties, such as mechanical strength, tensile strength and flexibility in biofilm applications. These suggest *A. paeoniifolius* starch a promising candidate for sustainable and biodegradable food packaging. These findings align with research by Julianti and coworkers (Julianti et al., 2018) which highlight the potential of *Amorphophallus* starch for developing eco-friendly biofilms with desirable mechanical and barrier characteristics, essential for sustainable packaging applications.

3.3. Fourier Transform Infrared Spectroscopy (FTIR) Spectral Analysis

FTIR spectroscopy was used to identify functional groups in the isolated starch from *A. paeoniifolius* by analysing peak values within the infrared region. This analysis provided insight into the structural characteristics of the starch. The obtained data is graphically represented in Fig. 1, which displays the FTIR spectrum of *A. paeoniifolius*, illustrating transmittance (%) as a function of wavenumber (cm^{-1}). A broad absorption band observed around 3000 cm^{-1} is attributed to O-H stretching vibrations, indicative of hydroxyl (–OH) groups and suggesting the presence of hydrogen bonding typically associated with starch and other polysaccharide compounds (Araújo et al., 2020; Abdullah et al., 2018). The peak at 2390 cm^{-1}, although rare in starch, may correspond to C≡C or C≡N triple bond stretching, potentially indicating trace

impurities or unique molecular interactions within the sample. A weak absorption band near 1870 cm^{-1} may be related to higher vibrations or minor C=O stretching, although such features are uncommon in standard starch profile (Araújo et al., 2020; Abdullah et al., 2018). Peaks at 1600 cm^{-1} and 1527 cm^{-1} are often associated with C=O stretching or N-H bending vibrations, characteristic of amide groups, which may indicate minimal protein residues retained from the starch extraction process. Bands around 1455 cm^{-1} and 1398 cm^{-1} likely correspond to C-H bending or scissoring vibrations, specifically linked to CH_2 groups. The absorption peak at 1270 cm^{-1} is attributed to C-O stretching vibrations, which are commonly observed in polysaccharides and indicative of glycosidic linkages within the starch structure. Additionally, peaks at 946 cm^{-1} and 889 cm^{-1} are consistent with C-O-C stretching, characteristic of glycosidic bonds and supportive of the polysaccharide framework typical of starch (Araújo et al., 2020; Abdullah et al., 2018). A band at 825 cm^{-1} may be associated with C-H out-of-plane bending, often representative of the polysaccharide backbone structure. The observed spectral features align with findings from (Julianti et al., 2018; Araújo et al., 2020; Abdullah et al., 2018), who reported similar absorption patterns in starch samples. This alignment supports the structural integrity and purity of *A. paeoniifolius* starch, reinforcing its suitability for further applications in food and biopolymer research.

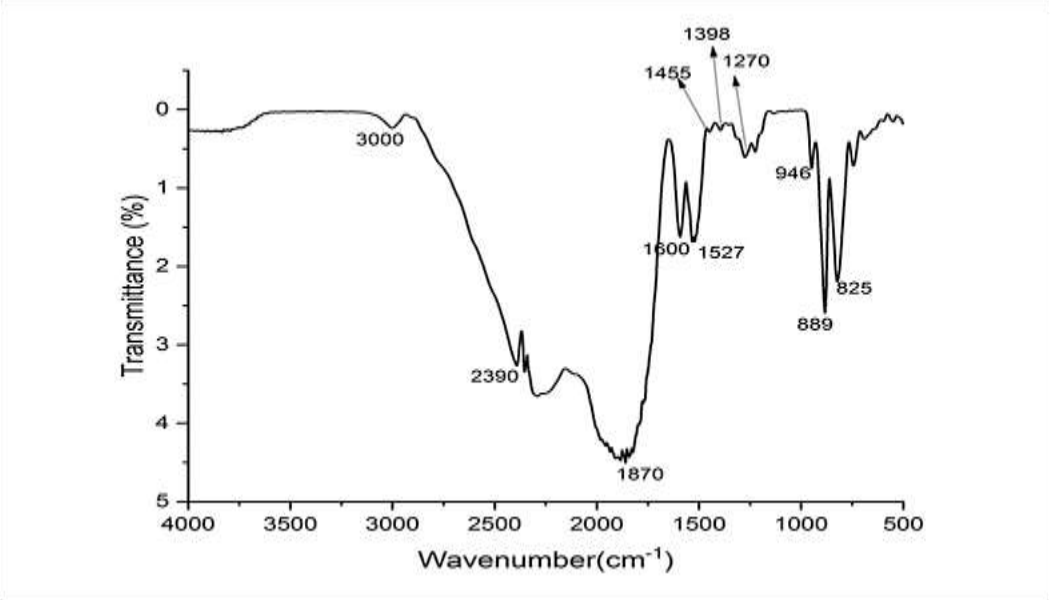

Fig. 1: FTIR spectra of *Amorphophallus paeoniifolius* starch showing characteristic absorption bands corresponding to functional groups.

3.4. Thermal Analysis of Starch Using Differential Scanning Calorimetry (DSC)

Gelatinization is a process in which starch undergoes structural breakdown when exposed to heat and moisture. This transformation begins with the hydration and swelling of the amorphous regions within the

starch granules, which induces stress on the crystalline regions, ultimately leading to their rupture and the melting of the granules. The peak temperature (Tp) at which this transition occurs is influenced by the structural arrangement and molecular composition of amylose and amylopectin within the starch matrix (Gupta & Gaur, 2024). The enthalpy change (ΔH), as measured by DSC, quantifies the heat absorbed during all endothermic events that occur during the heating process. Several factors, including moisture content, solvent type, degree of hydration, botanical origin, and physical granule properties, influence the ΔH values (Alonso-Gomez et al., 2016). Studies have shown that lower moisture content correlates with higher gelatinization temperatures, a significant factor in low-moisture systems such as baked goods or starch-based biofilm plasticization (Zuo et al., 2019).

The DSC thermogram of *A. paeonifolius* starch, shown in Fig. 2, provides valuable insights into its thermal properties, including the enthalpy change and melting temperature. The thermogram reveals an onset temperature of 106.4°C, where the thermal transition initiates, followed by the peak of the endothermic process at 114.8°C, and concluding at 126.7°C. The enthalpy change (ΔH) was measured to be 563 J/g. These results align with the thermal characteristics typically observed for starches and are consistent with findings reported by (Kandekar et al., 2021).Among various starches, potato starch has the lowest gelatinization temperature, around 62°C, while corn and cassava starches exhibit higher gelatinization temperatures, at approximately 66°C and 68°C, respectively (Gernat et al., 1990; Lumdubwong & Seib, 2000). Higher crystallinity generally contributes to greater thermal stability, which, in turn, raises the gelatinization temperature. This effect is further influenced by the amylopectin chain length. In bioplastic production, precise control of the gelatinization temperature is crucial. Temperatures below 60°C can result in premature gelatinization during drying, while excessively high temperatures increase energy costs (Abdullah et al., 2018).

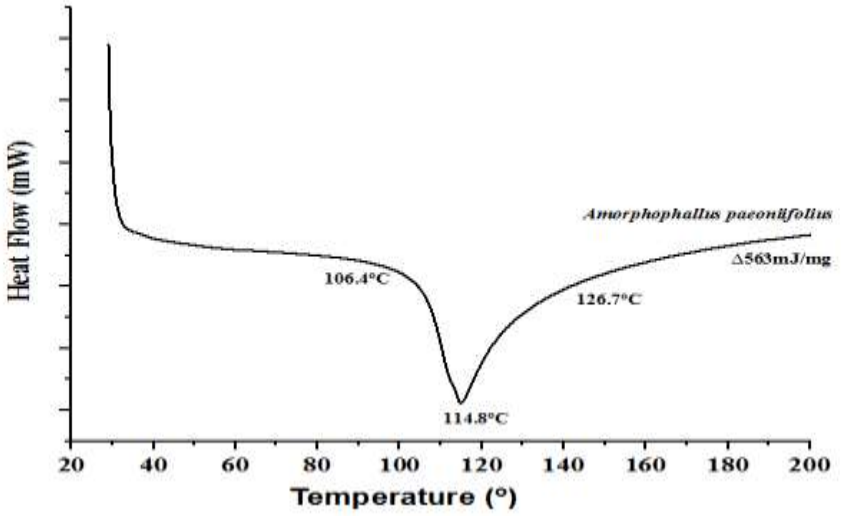

Fig. 2: Differential scanning calorimetry (DSC) curve of *Amorphophallus paeoniifolius* starch showing thermal transition during gelatinization**.**

3.5. Morphological Characterization of Starch Obtained from *A. Paeoniifolius* by Scanning Electron Microscopy (SEM)

The SEM is a highly versatile instrument widely used for examining microstructural morphology and characterizing the chemical composition of various materials (Zhou et al., 2007). SEM operates based on electron emission, providing high-resolution, gray-scale images that offer detailed insights into a sample's surface structure. Fig. 3A, 3B, and 3C presents scanning electron microscopy (SEM) micrographs of *A. paeoniifolius* starch granules at different magnifications (2.50 KX, 1.20 KX, and 3.25 KX, respectively), illustrating variations in morphology, size, and surface characteristics. Fig. 3A (2.50 KX magnification) offers a close-up of individual starch granules, revealing a morphological heterogeneity of *A. paeoniifolius* starch, with irregular, polygonal, rounded granules, variable sizes with predominantly smooth surfaces and occasional indentations. The variability in granule size observed here is typical of starches from diverse plant sources. Fig. 3B (1.20 KX magnification) provides a broader view of the granule distribution, displaying a clustering tendency that suggests inter-granular interactions. Such aggregation could potentially influence properties like water absorption and gelatinization, which are critical for certain applications. Fig. 3C (3.25 KX magnification) allows for a detailed examination of the granule surfaces, showcasing minor irregularities and reinforcing the diversity in shape and size, with granules ranging within the micrometer scale. The tight packing of granules suggests a natural tendency for aggregation, which may impact functional properties in food and biopolymer applications. Similar morphological diversity has been noted in prior studies, linking granule characteristics to plant origin (Sukhija et al., 2016). Granule size and shape, as well as clustering behavior, significantly influence physicochemical properties such as swelling power, light transmittance, water-binding capacity, and amylose content traits essential for functional applications (Cone & Wolters, 1990).

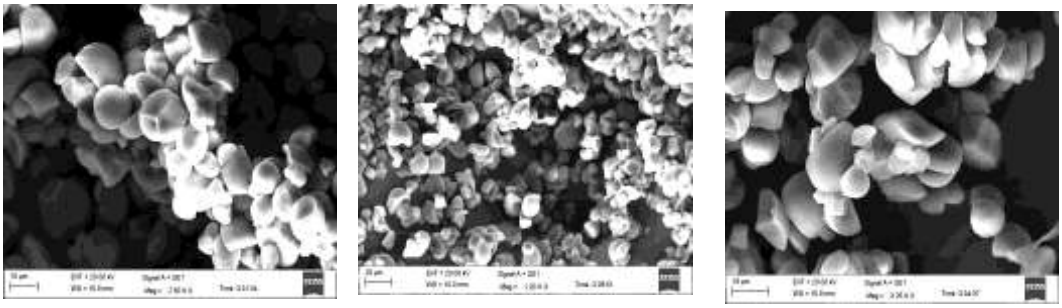

A B C

Fig. 3: SEM images of *Amorphophallus paeoniifolius* starch under different magnification (A) 2.50 K (B) 1.20 K (C) 3.25 K, depicting the morphology of starch granules.

3.6. Energy Dispersive X-ray Spectroscopy

Energy Dispersive X-ray Spectroscopy (EDS), used alongside SEM, is a powerful analytical technique for obtaining qualitative and semi-quantitative data on a sample's elemental composition (Mohammed & Abdullah, 2018).EDS enables the identification of elements within a specimen through advanced computer software, offering insights not accessible via conventional tests .Fig. 4 shows the EDS analysis of *A. paeoniifolius* starch revealing prominent peaks of carbon (C) and oxygen (O), which are characteristic of carbohydrate-rich substances. Based on quantitative data, the weight percentages (wt. %) of carbon and oxygen in starch are36.75% and 63.25%, respectively. These values are further confirmed by the normalized weight percentages. The atomic percentages reveal that oxygen has a slightly higher concentration at 56.37%, compared to carbon's 43.63%. The error margins associated with each element suggest a reasonable degree of accuracy in these measurements, although a higher error margin was noted for carbon at 22.3%. Similar compositional results have been reported by (Sukhija et al., 2016; Wahyuningtiyas & Suryanto, 2017), demonstrating a consistency of these findings.

The SEM image within the spectrum displays the granular morphology of the starch at high magnification. This morphological observation allows for a correlation between the structural characteristics and the elemental composition derived from EDS analysis, providing a more comprehensive understanding of the physicochemical properties of the starch. Such insights are crucial for evaluating the material's suitability for applications in biodegradable film production and food packaging, where both composition and structure play significant roles. It is important to note that EDS analysis primarily detects elements with atomic numbers above approximately 4–5. This limitation arises from the fundamental mechanism of EDS, which relies on detecting characteristic X-rays emitted when atoms are excited by an electron beam. Due to its low atomic number and lack of high-energy X-ray emissions, hydrogen (atomic number 1) remains undetectable in standard EDS. Consequently, only heavier elements, such as carbon and oxygen in *A. paeoniifolius* starch, are observable in the spectrum.

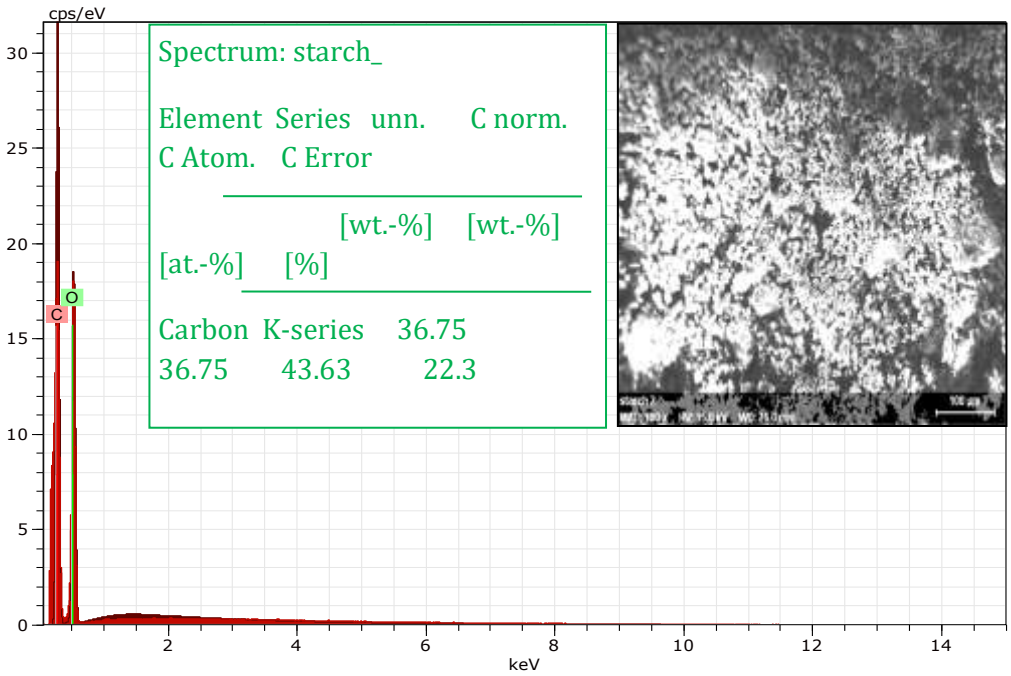

Fig. 4: EDX analysis of the *A.paeoniifolius* starch.

3.7. X-ray Structural Characterization

Within starch structure, amylopectin chains adopt a helical conformation due to coiling of glucose monomers. These helices intertwine to form double helices, which are systematically arranged, contributing to the crystalline nature of starch. Amylose and the branched regions of amylopectin play a crucial role in supporting this structural organization, primarily forming the amorphous regions of starch (Gupta & Gaur, 2024). The nanoscale structure of *A. paeoniifolius* starch was analyzed using X-ray Diffraction (XRD), as illustrated in Fig. 5. Indexing, a crucial step in structural characterization was used to determine the unit cell dimensions and arrangement based on the diffraction peaks. This process involved assigning Miller indices (h k l) to specific peaks, providing insight into the starch's crystal structure. In this study, the primary peak reflections identified were 112, 020, 013, 103, 121, 022, 123, and 213, as detailed in Table 2. These reflections reveal key structural aspects of the starch at the nanoscale. The broad peaks XRD profile indicates a small crystallite size, a typical feature of nanocrystalline materials, which influence properties relevant to biodegradable films and biopolymer applications.

Table2: Miller indexes, Bragg angles and inter plannar spacing of *Amorphophallus. paeoniifolius* starch

Miller indices (hkl)	2θ of peak(deg)	d-spacing (Ao)
112	14.80	5.9823
020	15.17	5.8373
013	16.80	5.2744
103	17.16	5.1645
121	17.90	4.9527
022	18.20	4.8717
123	22.92	3.8780
213	23.70	3.7521

The size of the starch particles was calculated using the Debye-Scherrer formula, as referenced in studies by (Marimuthu et al., 2013; Theivasanthi &Alagar, 2011). Particle size and distribution are critical characteristics in particle systems, as these factors influence the in vivo distribution, biological behavior, toxicity, and targeting efficiency of the particles. Research has consistently demonstrated that particles in the sub-micron range offer significant advantages over microparticles, particularly as drug delivery systems, due to their enhanced bioavailability and targeted delivery potential by (Marimuthu et al., 2013; Theivasanthi &Alagar, 2011). To determine the average particle size, the Debye-Scherrer equation was applied (equation 2), which is commonly used to estimate crystallite sizes based on the broadening of X-ray diffraction peaks.

$$D = \frac{K\lambda}{\beta Cos\theta} \qquad (2)$$

Here, 'D' is the average particle size, 'K' is the shape factor (typically around 0.9 for spherical particles), 'λ' is the X-ray wave length (usually 0.1541 nm), 'β' is the full width at half maximum (FWHM) of the diffraction peak (in radians), and 'θ' is the Bragg angle. The calculated particle size data is presented in Table 3. Additionally, the inter planar spacing'd', which represents the distance between atomic planes, was calculated using Bragg's Law (equation 3). This approach offers a comprehensive understanding of the structural characteristics of *A. paeoniifolius* starch particles, allowing for a more precise evaluation of their potential applications in fields such as biomedicine and materials science.

$$2d\sin\theta = n\lambda \qquad (3)$$

Table3: Grain size of *Amorphophallus. paeoniifolius* starch from XRD

2θ of peak (deg)	Miller indices (hkl)	FWHM (Full Width at Half Maximum) peak (β) (radians)	Size of particle (D) nm	d- spacing (nm)	d- spacing (Å)
14.80	112	0.0145	9.9043	0.5982	5.9823
15.17	020	0.0099	14.4470	0.5837	5.8373
16.80	013	0.0140	10.3777	0.5274	5.2744
17.16	103	0.0131	11.0908	0.5165	5.1645
17.90	121	0.0129	11.2867	0.4953	0.49527
18.20	022	0.0171	8.5371	0.4872	4.8717
22.92	123	0.0187	8.0646	0.3878	3.8780
23.70	213	0.0201	7.5577	0.3752	3.7521

3.8. XRD-Starch Analysis and Quantification of Crystallinity

The XRD analysis of the sample revealed a B-type diffraction pattern, characteristic of crystalline starch structures commonly observed in tuber starches. Intermediate intensity peaks at 2θ angles of 17.52° and 18.22° align with this pattern, consistent with findings by (Zobel, 1988). Additionally, a prominent peak appears at 2θ = 23.12°, and a less pronounced hump at 15.01° resembles an A-type diffraction pattern, typically associated with cereal starches. Interestingly, EFY starch displayed a C-type diffraction pattern, a hybrid of A and B types, which contrasts with results reported by (Reddy et al., 2014). Both A- and B-type starches exhibit identical double helices but differ in their packing arrangement and moisture content. The A-type crystalline structure is characterized by densely packed helices, typically accommodating four water molecules. In contrast, the B-type structure adopts a more open hexagonal arrangement, incorporating up to 36 water molecules. These diffraction patterns are influenced by factors such as amylopectin chain length, amylose content, and the biological source of the starch, as noted by (Saikia and Konwar, 2012). From a crystallographic perspective, starch has been observed to exhibit two primary crystal structures: orthorhombic and hexagonal. Rodriguez-García et al., 2021 reported that starches with an orthorhombic arrangement are classified as A-type, while those with a hexagonal structure are labeled as B-type. Starches that exhibit a combination of these structures are classified as C-type (Esquivel-Fajardo et al., 2022). The XRD pattern of the *A. paeoniifolius* starch in this study indicates the presence of both hexagonal and orthorhombic crystal structures, thereby categorizing it as C-type, as depicted in Fig. 5. The pattern of

coexistence of both structural types within its crystalline regions aligns with the finding reported by Dioscorea species (Jiang et al., 2012).

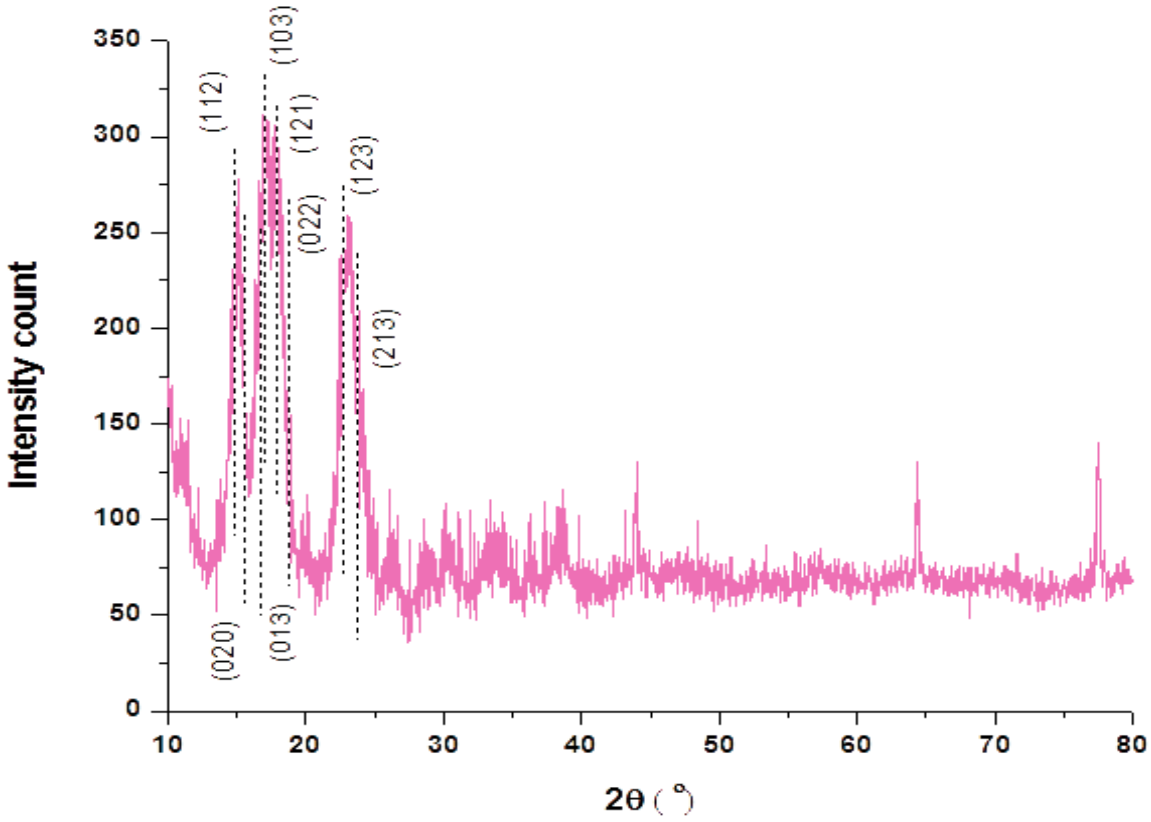

Fig. 5: X-Ray diffraction (XRD) pattern of *Amorphophallus.paeoniifolius* starch**.**

Quantifying the degree of crystallinity is a key application of XRD, especially valuable for materials that contain both crystalline and amorphous phases. It is classified as a semi-crystalline polymer, with its crystalline regions mainly attributed to amylose and amorphous regions of amylopectin. XRD analysis in this study revealed a calculated relative crystallinity of 34.3% for *A. paeoniifolius* starch, a result that aligns closely with previous literature findings (Jiang et al., 2012). Further comparisons with other starches revealed that Yam Starch (YS) and Taro Starch (TS) exhibited crystallinity levels of 32.88% and 44.66%, respectively (Andrade et al., 2017).

3.9. XRD-Specific Surface Area and Morphology Index

A. paeoniifolius starch powder is widely utilized across multiple industries, including the food industry, pharmaceuticals, drug delivery, cosmetics, and the paper. The specific surface area (SSA) of the amorphous starch powder is suggested to be determined by the relationship between particle size and the

morphology index (MI), as presented in Table 4. The MI is calculated based on the full width at half maximum (FWHM) values obtained from XRD data and provides a quantitative measure of particle morphology, consequently its SSA.

The MI is defined as the ratio between the FWHM value of the peak with the greatest intensity and the FWHM value of a specific reference peak. This provides a quantitative measure of particle morphology, which is outlined by the following equation 4:

$$M.I = \frac{FWHMh}{FWHMh+FWHMp} \quad (4)$$

Where, $FWHM_h$ is highest FWHM value, and FWHMp is FWHM value of a particular peak, (Theivasanthi & Alagar, 2011). This index aids in correlating particle size and shape, crucial factors in understanding the starch's applications across various industries. Experimental MI value for *A. paeoniifolius* starch powder ranged from 0.50 to 0.67, as shown in Table 4. A strong positive correlation was observed between MI and particle size i.e. MI increases, particle size also tends to increase, while MI showed a near-perfect negative correlation with SSA i.e. MI increases, SSA decreases. The SSA is a fundamental property of materials, providing critical insights into material identification and characterization. SSA denotes the surface area available per unit mass and is particularly significant in applications involving adsorption, heterogeneous catalysis, and surface-related reactions. This parameter is essential in assessing materials for various industrial and scientific applications, as it influences their reactivity, stability, and effectiveness in specific roles. It is calculated using the formula presented in equation 5:

$$S = \frac{6*10^3}{Dp\ \rho}, \quad (5)$$

Where, S represents the specific surface area (SSA), Dp denotes the particle size, and ρ signifies the density of *A. paeoniifolius* starch, which has been measured at 0.8 grams per cubic centimeter. This relationship is instrumental in calculating SSA, as it accounts for both particle size and material density, thereby providing a comprehensive assessment of surface area per unit mass.

Table 4: Morphology index &specific surface area of *A. paeoniifolius* particles.

FWHM (Full Width at Half Maximum) (β) (radians)	**Particle Size (D) (nm)**	**Morphology Index**	**SSA (m2/g)**
0.0145	9.9043	0.5808	757.2456
0.0099	14.4470	0.6686	519.138
0.0140	10.3777	0.5897	722.7006

0.0131	11.0908	0.6053	676.2332
0.0129	11.2867	0.6085	664.5002
0.0171	8.5371	0.5399	878.5135
0.0187	8.0646	0.5180	929.9901
0.0201	7.5477	0.5000	993.6761

4. CONCLUSIONS

This study comprehensively evaluated the physicochemical properties of *A. paeoniifolius* starch, a less-explored tropical tuber, highlighting its potential as a sustainable material for bioplastics and food packaging. Characterization using DSC, FTIR, XRD, SEM, and EDX indicates the starch's potential suitability for producing biodegradable films. The results show that *A. paeoniifolius* starch exhibit stable thermal properties, molecular integrity, and a semi-crystalline structure, with a crystallinity index of 34.3%. Proximate composition analysis revealed a high starch content of 78.61%, moisture content of 11.8%, and low-fat content (0.30%), suggesting its viability as a carbohydrate- rich raw material. However, direct testing of film-forming ability and mechanical performance was not conducted in this study. Preliminary findings suggest that, with further optimization, this starch could be used in biodegradable packaging applications. Future research should optimize film preparation and processing to improve mechanical, barrier, and thermal properties for large-scale applications.

Author Contributions: Conceptualization, N.S., N.W., and S.G; methodology, N.S.; software, N.S.; validation, N.S., N.W., and S.G.; formal analysis, N.S; investigation, N.S; resources, N.W. and S.G.; data curation, N.S.; writing—original draft preparation, N.S.; writing—review and editing, N.W. and S.G.; visualization, N.S., N.W., and S.G.; supervision, N.W. and S.G. All authors have read and agreed to the published version of the manuscript.

Funding: This research received no external funding

Acknowledgment: The authors are grateful to the Department of Biotechnology, Jaypee Institute of Information Technology, Noida, Uttar Pradesh, India for providing necessary facilities to execute this work.

Conflicts of Interest: The authors declare that they have no conflicts of interest.

REFERENCES

1. Abbas, K.A., Khalil, S.K., & Hussin, A.S.M, 2010. Modified starches and their usages in selected food products: A review study. *Journal of Agricultural Science*, *2*(2), pp. 90. https://doi.org/10.5539/jas.v2n2p90

2. Abdullah, A.H.D., Chalimah, S., Primadona, I., & Hanantyo, M. H. G., 2018. Physical and chemical properties of corn, cassava, and potato starchs. *IOP Conference Series. Earth and Environmental Science*, *160*, 012003. https://doi.org/10.1088/1755-1315/160/1/012003
3. Abegunde, O. K. 2012. Physicochemical characterization of starches from some Nigerian and Chinese roots and tubers. *African Journal of Food Science*, *6*(11). https://doi.org/10.5897/ajfs12.048
4. Alinnor, I. J., & Akalezi, C. O., 2010. Proximate and Mineral Compositions of Dioscorea rotundata (White Yam) and Colocasia esculenta (White Cocoyam). *Pakistan Journal of Nutrition : PJN*, *9*(10), 998–1001. https://doi.org/10.3923/pjn.2010.998.1001
5. Alonso-Gomez, L., Niño-López, A. M., Romero-Garzón, A. M., Pineda-Gomez, P., del Real-Lopez, A., & Rodriguez-Garcia, M. E., 2016. Physicochemical transformation of cassava starch during fermentation for production of sour starch in Colombia: Transformation of cassava starch during fermentation. *Die Starke*, *68*(11–12), 1139–1147. https://doi.org/10.1002/star.201600059
6. Alozie, Y. E., Iyam, M. A., Lawal, O., Udofia, U., & Ani, I. F., 2009. *Utilization of Bambara Groundnut Flour blends in bread production Journal of food technology, 7(4), 111-114*.
7. Andrabi, S. N., Wani, I. A., Gani, A., Hamdani, A. M., & Masoodi, F. A., 2016. Comparative study of physico-chemical and functional properties of starch extracted from two kidney bean (*Phaseolus vulgaris* L.) and green gram cultivars (*Vigna radiata* L.) grown in India. *Starch-Stärke*, *68*(5–6), 416–426.
8. Andrade, L. A., Barbosa, N. A., & Pereira, J., 2017. Extraction and properties of starches from the non-traditional vegetables Yam and Taro. *Polímeros*, *27*(2), 151–157. https://doi.org/10.1590/0104-1428.04216
9. Galvão A.M.M.T, de Oliveira Araújo, A. W., Carneiro, S. V., Zambelli, R. A., & Bastos, M.D.S.R., 2018. Coating development with modified starch and tomato powder for application in frozen dough. *Food Packaging and Shelf Life*, *16*, 194–203. https://doi.org/10.1016/j.fpsl.2018.04.003
10. Aprianita, A., Purwandari, U., Watson, B., & Vasiljevic, T., 2009. Physico-chemical properties of flours and starches from selected commercial tubers available in Australia. *International Food Research Journal*, *16*(4), 507–520.
11. Araújo, R. G., Rodríguez-Jasso, R. M., Ruiz, H. A., Govea-Salas, M., Rosas-Flores, W., Aguilar-González, M. A., Pintado, M. E., Lopez-Badillo, C., Luevanos, C., & Aguilar, C. N., 2020. Hydrothermal–microwave processing for starch extraction from Mexican avocado seeds: Operational conditions and characterization. *Processes (Basel, Switzerland)*, *8*(7), 759. https://doi.org/10.3390/pr8070759
12. Ashaolu, T. J. (2020). Soy bioactive peptides and the gut microbiota modulation. *Applied Microbiology and Biotechnology*, *104*(21), 9009–9017. https://doi.org/10.1007/s00253-020-10799-2
13. Awuchi, C. G., Chukwu, C. N., Iyiola, A. O., Noreen, S., Morya, S., Adeleye, A. O., Twinomuhwezi, H., Leicht, K., Mitaki, N. B., & Okpala, C. O. R., 2022. Bioactive compounds and therapeutics from fish: Revisiting their suitability in functional foods to enhance human wellbeing. *BioMed Research International*, *2022*, 3661866. https://doi.org/10.1155/2022/3661866

14. Boahemaa, L. V., Dzandu, B., Amissah, J. G. N., Akonor, P. T., & Saalia, F. K., 2024. Physico-chemical and functional characterization of flour and starch of taro (Colocasia esculenta) for food applications. *Food and Humanity*, *2*(100245), 100245. https://doi.org/10.1016/j.foohum.2024.100245
15. Cone, J. W., & Wolters, M. G. E., 1990. Some properties and degradability of isolated starch granules. *Die Starke*, *42*(8), 298–301. https://doi.org/10.1002/star.19900420804
16. Cummings, J. H., & Stephen, A. M., 2007. Carbohydrate terminology and classification. *European Journal of Clinical Nutrition*, *61 Suppl 1*(S1), S5-S18. https://doi.org/10.1038/sj.ejcn.1602936
17. Esquivel-Fajardo, E. A., Martinez-Ascencio, E. U., Oseguera-Toledo, M. E., Londoño-Restrepo, S. M., & Rodriguez-García, M. E., 2022. Influence of physicochemical changes of the avocado starch throughout its pasting profile: Combined extraction. *Carbohydrate Polymers*, *281*(119048), 119048. https://doi.org/10.1016/j.carbpol.2021.119048
18. Geirnaert, A., Calatayud, M., Grootaert, C., Laukens, D., Devriese, S., Smagghe, G., De Vos, M., Boon, N., & Van de Wiele, T., 2017. Butyrate-producing bacteria supplemented in vitro to Crohn's disease patient microbiota increased butyrate production and enhanced intestinal epithelial barrier integrity. *Scientific Reports*, *7*(1), 11450. https://doi.org/10.1038/s41598-017-11734-8
19. Gernat, C., Radosta, S., Damaschun, G., & Schierbaum, F., 1990. Supra molecular structure of legume starches revealed by X-ray scattering. *Die Starke*, *42*(5), 175–178. https://doi.org/10.1002/star.19900420504
20. Gupta, R., & Gaur, S. 2024. Investigating the effect of natural fermentation in modifying the physico-functional, structural and thermal characteristics of pearl and finger millet starch. *Journal of the Science of Food and Agriculture*, *104*(4), 2440–2448. https://doi.org/10.1002/jsfa.13129
21. Hamaker, B. R., & Griffin, V. K., 1993. *Effect of disulfide bond-containing protein on rice starch gelatinization and pasting*. *Cereal Chemistry* 70(4), 377–380.
22. He, Y., Wang, B., Wen, L., Wang, F., Yu, H., Chen, D., Su, X., & Zhang, C., 2022. Effects of dietary fiber on human health. *Food Science and Human Wellness*, *11*(1), 1–10. https://doi.org/10.1016/j.fshw.2021.07.001
23. Huang, H., Krishnan, H. B., Pham, Q., Yu, L. L., & Wang, T. T. Y., 2016. Soy and gut Microbiota: Interaction and implication for human health. *Journal of Agricultural and Food Chemistry*, *64*(46), 8695–8709. https://doi.org/10.1021/acs.jafc.6b03725
24. Ijarotimi, O. S., Fagbemi, T. N., & Osundahunsi, O. F., 2015. Evaluation of nutrient composition, glyceamic index and anti-diabetic potentials of multi-plant based functional foods in rats. *Sky Journal of Food Science*, *4*(6), 78–90.
25. *Indian standard, 2022 .Infant Food - Milk-Cereal Based Complementary Foods- Specification*, (IS 1656:2022).
26. *Indian standard, 1981. Specification for Ready-to-Protein-Rich Extruded Foods,(*IS 9487:1981*)*
27. Indian standard 2019 Method for Estimation of Total Dietary Fibre in Foodstuffs,(IS 11062:2019.). *Bureau of Indian Standards (BIS). Govt. of India*.
28. *Indian Standard,* 1975. *Specification for Bombay Halwa Bureau of Indian Standards*,(2650:1975).

29. Islam, F., Noman, M., Afzaal, M., Saeed, F., Ahmad, S., Zubair, M. W., Zahra, S. M., Hussain, M., Ateeq, H., & Awuchi, C. G., 2022. Synthesis and food applications of resistant starch-based nanoparticles. *Journal of Nanomaterials*, *2022*(1). https://doi.org/10.1155/2022/8729258
30. Jiang, Q., Gao, W., Li, X., Xia, Y., Wang, H., Wu, S., Huang, L., Liu, C., & Xiao, P., 2012. Characterizations of starches isolated from five different Dioscorea L. species. *Food Hydrocolloids*, *29*(1), 35–41. https://doi.org/10.1016/j.foodhyd.2012.01.011
31. Jubril, I., Muazu, J., & Mohammed, G. T., 2012. Effects of phosphate modified and pregelatinized sweet potato starches on disintegrant property of paracetamol tablet formulations. *Journal of Applied Pharmaceutical Science*, 32–36.
32. Julianti, E., Rusmarilin, H., Ridwansyah, &Yusraini, E., 2018. Effect of isolation methods on physicochemical properties of purple-fleshed sweet potato starch. *Proceedings of the International Conference of Science, Technology, Engineering, Environmental and Ramification Researches (ICOSTEERR 2018)-Research in Industry, 4, 37-41.*
33. Kale, R. V., Shere, D. M., Sontakke, M. D., & Gadhe, K. S., 2017. Effect of isolation methods on physicochemical and functional properties of sweet potato (Ipomoea batatas L.) starch. *Journal of Pharmacognosy and Phytochemistry*, *6*(4), 223–227.
34. Kandekar, U. Y., Abhang, T. R., Pujari, R. R., & Khandelwal, K.R., 2021. Exploration of elephant foot yam (*Amorphophallus paeoniifolius*) starch: An alternative natural disintegrant for pharmaceutical application. *Indian Journal of Pharmaceutical Education*, *55*(1s), s209–s219. https://doi.org/10.5530/ijper.55.1s.52
35. Kaur, M., & Sandhu, K. S., 2010. Functional, thermal and pasting characteristics of flours from different lentil (Lens culinaris) cultivars. *Journal of Food Science and Technology*, *47*(3), 273–278. https://doi.org/10.1007/s13197-010-0042-0
36. Kibret Akalu, Z., & Haile Geleta, S., 2019. Comparative analysis on the proximate composition of tubers of *Colocasia esculenta, L. schott* and *Dioscore aalata* cultivated in Ethiopia. *American Journal of Bioscience and Bioengineering*, *7*(6), 93. https://doi.org/10.11648/j.bio.20190706.13
37. Levitsky, A. P., Egorov, B. V., Lapinskaya, A. P., & Selivanskaya, I. A., 2020. Inadequate fat diet. *Journal of Education, Health and Sport*, *10*(7), 248–255. https://doi.org/10.12775/jehs.2020.10.07.029
38. Liang, X., & King, J. M., 2003. Pasting and crystalline property differences of commercial and isolated rice starch with added amino acids. *Journal of Food Science*, *68*(3), 832–838. https://doi.org/10.1111/j.1365-2621.2003.tb08251.x
39. Lumdubwong, N., & Seib, P. A., 2000. Rice starch isolation by alkaline protease digestion of wet-milled rice flour. *Journal of Cereal Science*, *31*(1), 63–74. https://doi.org/10.1006/jcrs.1999.0279
40. M,S., ChagamKoteswara, R., Sundaramoorthy, H., & N, H., 2018. Influence of debranching and retrogradation time on behavior changes of *Amorphophallus paeoniifolius* nanostarch. *International Journal of Biological Macromolecules*, *120*(Pt A), 230–236. https://doi.org/10.1016/j.ijbiomac.2018.08.059

41. Marichelvam, M. K., Jawaid, M., &Asim, M., 2019. Corn and rice starch-based bio-plastics as alternative packaging materials. *Fibers (Basel, Switzerland)*, *7*(4), 32. https://doi.org/10.3390/fib7040032
42. Marimuthu, M., Sundaram, U., & Gurumoorthi, P., 2013. X-ray diffraction and starch analysis of nano-sized seed powder of velvet bean (Mucunapruriens). *Indo American Journal of Pharmaceutical Research*, *3*(2).
43. Meludu, N. T., 2010. Proximate analysis of Sweet potato toasted granules. *African Journal of Biomedical Research*, *13*(1), 89–91.
44. Methods of tests for edible starches and starch products. 1978. *Bureau of Indian Standards (BIS)*, *4706:1978*.
45. Mohammed, A., & Abdullah, A., 2018. Scanning electron microscopy (SEM): A review. In *Proceedings of the 2018 International Conference on Hydraulics and Pneumatics-HERVEX* (pp. 7–9).
46. Mukherjee, A., Banerjee, A., Sinhababa, A., & Singh, P. P., 2014. The genus Amorphophallus: Cyto-histo-molecular genesis and commercial prospects. *International Journal of Innovative Horticulture*, *3*, 12–21.
47. Olkku, J., & Rha, C., 1978. Gelatinisation of starch and wheat flour starch—A review. *Food Chemistry*, *3*(4), 293–317. https://doi.org/10.1016/0308-8146(78)90037-7
48. Omar, K. A., Salih, B. M., Abdulla, N. Y., Hussin, B. H., & Rassul, S. M., 2016. Evaluation of starch and sugar content of different rice samples and study their physical properties. *Indian Journal of Natural Sciences*, *6*(36), 11084–11088.
49. Omodamiro, R. M., Afuape, S. O., Njoku, C. J., Nwankwo, I. I. M., Echendu, T. N. C., & Edward, T. C., 2013. Acceptability and proximate composition of some sweet potato genotypes: Implication of breeding for food security and industrial quality. *International Journal of Biotechnology and Food Science*, *1*(5), 97–101.
50. Oyom, W., Zhang, Z., Bi, Y., &Tahergorabi, R., 2022. Application of starch-based coatings incorporated with antimicrobial agents for preservation of fruits and vegetables: A review. *Progress in Organic Coatings*, *166*(106800), 106800. https://doi.org/10.1016/j.porgcoat.2022.106800
51. Özdamar, E. G., & Ateş, M., 2018. *Rethinking sustainability: A research on starch based bioplastic*. *3*, 249–260.
52. Reddy, C. K., Haripriya, S., Noor Mohamed, A., & Suriya, M., 2014. Preparation and characterization of resistant starch III from elephant foot yam (*Amorphophallus paeonifolius*) starch. *Food Chemistry*, *155*, 38–44. https://doi.org/10.1016/j.foodchem.2014.01.023
53. Rodriguez-Garcia, M. E., Hernandez-Landaverde, M. A., Delgado, J. M., Ramirez-Gutierrez, C. F., Ramirez-Cardona, M., Millan-Malo, B. M., &Londoño-Restrepo, S. M., 2021. Crystalline structures of the main components of starch. *Current Opinion in Food Science*, *37*, 107–111. https://doi.org/10.1016/j.cofs.2020.10.002
54. Saikia, J. P., & Konwar, B. K., 2012. Physicochemical properties of starch from aroids of North East India. *International Journal of Food Properties*, *15*(6), 1247–1261. https://doi.org/10.1080/10942912.2010.491929
55. Schoch, T. J., 1968. Preparation and properties of various legume starches. *Cereal Chem*, *45*, 564–573.
56. Shujun, W., Jinglin, Y., & Wenyuan, G., 2005. Use of X-ray diffractometry (XRD) for identification of Fritillaria according to geographical origin. *American Journal of Biochemistry & Biotechnology*, *1*(4), 207–211. https://doi.org/10.3844/ajbbsp.2005.207.211

57. Shujun, W., Wenyuan, G., Hongyan, L., Haixia, C., Jiugao, Y., & Peigen, X., 2006. Studies on the physicochemical, morphological, thermal and crystalline properties of starches separated from different Dioscoreaopposita cultivars. *Food Chemistry*, *99*(1), 38–44. https://doi.org/10.1016/j.foodchem.2005.07.007
58. Singh, A., & Wadhwa, N., 2014. A review on multiple potential of aroid: *Amorphophallus paeoniifolius*. Int J Pharm Sci Rev Res, 24(1), 55–60
59. Sondari, D., Falah, F., Suryaningrum, R., Sari, F. P., Sari, F. P., Septefani, A. A., Septefani, A. A., Restu, W. K., Restu, W. K., Sampora, Y., &Sampora, Y., 2019. Biofilm based on modified sago starch: Preparation and characterization. *REAKTOR*, *19*(3), 125–130. https://doi.org/10.14710/reaktor.19.3.125-130
60. Standard, I. 1973. *Method of determination of protein in foods and feeds*. 7219:1973.
61. Standard, I., 1975. *Specification for edible groundnut flour (expeller-pressed)*. *4684:1975*.
62. Sukhija, S., Singh, S., &Riar, C. S., 2016. Isolation of starches from different tubers and study of their physicochemical, thermal, rheological and morphological characteristics: Characterization of tuber starches. *Die Starke*, *68*(1–2), 160–168. https://doi.org/10.1002/star.201500186
63. Theivasanthi, T., & Alagar, M., 2011. An insight analysis of nano sized powder of jackfruit seed. *Nano Biomedicine and Engineering*, *3*(3). https://doi.org/10.5101/nbe.v3i3.p163-168
64. Titov, V. N., 2012. Regulation of insulin fatty acid metabolism, and then glucose in the implementation of the biological function of locomotion. *Clinical Laboratory Diagnosis*, *5*, 3–12.
65. Wahyuningtiyas, N. E., & Suryanto, H., 2017. Analysis of biodegradation of bioplastics made of cassava starch. *Journal of Mechanical Engineering Science and Technology*, *1*(1), 24–31. https://doi.org/10.17977/um030v1i12017p024
66. Witek, K., Wydra, K., & Filip, M., 2022. A high-sugar diet consumption, metabolism and health impacts with a focus on the development of substance use disorder: A narrative review. *Nutrients*, *14*(14), 2940. https://doi.org/10.3390/nu14142940
67. Yusuf, F., Kubo, A. I., Abdulrashid, F. U., Madu, S. J., & Muazu, J., 2022. Studies on the Physicochemical Properties of Coprocessed Starch obtained from Ipomoea batatas. *Nigerian Journal of Basic & Applied Sciences*, *2*. https://doi.org/10.4314/njbas.v30i2.5
68. Zhang, S., Fan, X., Lin, L., Zhao, L., Liu, A., & Wei, C., 2017. Properties of starch from root tuber of Stephania epigaea in comparison with potato and maize starches. *International Journal of Food Properties*, *20*(8), 1740–1750. https://doi.org/10.1080/10942912.2016.1217879
69. Zhou, W., Apkarian, R., Wang, Z. L., & Joy, D., 2007. *Scanning microscopy for nanotechnology: techniques and applications*. 1–40.
70. Zobel, H. F., 1988. Starch crystal transformations and their industrial importance. *Die Starke*, *40*(1), 1–7. https://doi.org/10.1002/star.19880400102
71. Zuo, Y., He, X., Li, P., Li, W., & Wu, Y., 2019. Preparation and characterization of hydrophobically grafted starches by in situ solid phase polymerization. *Polymers*, *11*(1), 72. https://doi.org/10.3390/polym11010072